General Becker–Döring equations: effect of dimer interactions

2002 J. Phys. A: Math. Gen. 35 3183

(http://iopscience.iop.org/0305-4470/35/14/303)

INSTITUTE OF PHYSICS PUBLISHING JOURNAL OF PHYSICS A: MATHEMATICAL AND GENERAL

J. Phys. A: Math. Gen. **35** (2002) 3183–3202 PII: S0305-4470(02)32900-7

General Becker–Döring equations: effect of dimer interactions

Colin D Bolton and Jonathan A D Wattis

Division of Theoretical Mechanics, School of Mathematical Sciences, Nottingham University, University Park, Nottingham NG7 2RD, UK

E-mail: pmxcb@maths.nottingham.ac.uk and Jonathan.Wattis@nottingham.ac.uk

Received 21 January 2002, in final form 21 February 2002
Published 29 March 2002
Online at stacks.iop.org/JPhysA/35/3183

Abstract

The effect of dimer (two-particle) interactions on the Becker–Döring model of nucleation is investigated. Initially we consider the problem with size-independent aggregation and fragmentation coefficients and a constant monomer concentration. Either an equilibrium or a steady-state solution is found: the former when fragmentation is stronger than aggregation, the latter otherwise. By employing asymptotic techniques, the manner in which the system reaches these states is examined. The dimer interaction is found to accelerate the system towards the equilibrium solution, but has little impact on the relaxation time to the steady-state solution. In cases where aggregation is dominant, the steady-state cluster size distribution can only be determined consistently when the manner of approach to steady state is also known. In the terminology of asymptotic methods, one needs to know the first correction term in order to deduce the leading-order solution. We show how this can be derived and so at steady state we find a flux of matter to larger aggregation numbers due to monomer interactions, with a small and decreasing reverse flux due to dimer interactions. We then consider the case of constant density, that is allowing the monomer concentration to vary, and investigate the effect of a strong dimer interaction on the convergence to equilibrium. Two timescales are present and each one is investigated. We determine the intermediate meta-stable state, the final state and the timescales over which the system relaxes into these states. All results are shown to agree with numerical simulations.

PACS numbers: 64.60.Qb, 02.70.Ns, 82.20.−w, 05.20.−y, 05.70.Ln

1. Introduction

Becker and Döring presented an enduring model of nucleation in 1935 [1]; clusters form by the addition, or subtraction, of single particles (monomers) with no interaction between

larger clusters. Such larger clusters evolve by maintaining a dynamic balance of monomer aggregation and fragmentation. This process is modelled as a chemical reaction; denoting an r-sized cluster by C_r, we have the reversible reaction

$$C_r + C_1 \rightleftharpoons C_{r+1}. \tag{1}$$

For each reaction there are two reaction rates to prescribe: we denote the forward rate by a_r and the reverse by b_{r+1}, both non-negative. Defining J_r as the net flux from cluster size r to $r+1$ and $c_r(t)$ as the concentration of clusters C_r at time t, we express the system by

$$\dot{c}_1 = 0 \tag{2}$$

$$\dot{c}_r = J_{r-1} - J_r \qquad r \geqslant 2 \tag{3}$$

$$J_r = a_r c_r c_1 - b_{r+1} c_{r+1} \qquad r \geqslant 1 \tag{4}$$

where we assume $\dot{c}_1 = 0$, in the spirit of the original formulation [1]. Later Penrose [2] generalized these equations by allowing the monomer concentrations to vary; this ensures the conservation of density

$$\rho = \sum_{r=1}^{\infty} r c_r. \tag{5}$$

These modified equations (3)–(5) are still referred to as the Becker–Döring equations. For certain aggregation and fragmentation rates the existence and uniqueness of a solution to (2)–(4) have been demonstrated by Ball *et al* [3] for densities below a critical value; furthermore, this result was subsequently generalized to arbitrary initial data by Ball and Carr [4]. The asymptotic solution for size-independent aggregation, and fragmentation, rates has been described by Wattis and King [5]. Such is the rich structure of the Becker–Döring equations that various aspects have been investigated, including the existence of meta-stable solutions by Penrose [6], the aggregation-dominated regime by Carr [7] and the difficulties in numerically modelling such meta-stable systems by Carr *et al* [8] and Duncan and Soheili [9]. The modelling of nucleation has proved to be applicable to a variety of circumstances such as the self-replication of micelles and vesicles [10, 11], and the origin of RNA, which have been studied by Coveney and Wattis [12] . Additional applications have been competitive nucleation [13], transitional aggregation kinetics [14], the role of chemical inhibitors [15] and monomer–monomer catalysis [16]. While being widely applicable, the Becker–Döring equations make the restrictive assumption that only monomers may interact with clusters. Smoluchowski [17] proposed a more general model allowing all cluster sizes to aggregate, and for a cluster to split into uneven fragments. Blackman and Marshall [18] exploited the Smoluchowski equations to study scaling behaviour in essentially the Becker–Döring regime, while Brilliantov and Krapivsky [19] have used a similar approach to study the problem of nucleation with movable monomers and immovable clusters.

Molecular dynamic simulations by Wonczak [20] on the condensation of argon suggest that while monomer interactions dominate the dynamics, dimer (two-particle clusters) interactions account for approximately 5% of all interactions. We follow the work of da Costa [21] in analysing a model which allows not only monomer, but additionally dimer interactions, which is a generalization of the Becker–Döring model. As an example we assume size-independent aggregation and fragmentation coefficients, $a_r = a$, $b_r = b$. The methods used in this paper closely follow those employed by Wattis and King [5]. The model studied then falls between that proposed by Smoluchowski and that by Becker and Döring, being more complicated than the latter but simpler than the former.

This introduction concludes with a description of the general dimer problem, from which we will extract particular cases to be studied. Section 2 begins by formulating the Becker–Döring system that has been investigated and proceeds to describe the equilibrium solution, where fragmentation dominates. Furthermore, we analyse the approach to this equilibrium state, including a description of the far-field asymptotics, and finish the section by analysing the behaviour of the Lyapunov function. In section 3 we consider the regime where aggregation dominates fragmentation, leading to a time-independent solution in which a material continuously aggregates into increasingly large cluster sizes. We construct the time-independent solution and describe the approach to this state and verify consistency with the far-field asymptotics. The constant density Becker–Döring system is then investigated in section 4, in the special case of a large dimer interaction; Maillet *et al* [23] reported on molecular dynamic simulations of cationic surfactants which form micelles with a strong contribution from the dimer interaction. The paper concludes with a discussion of the results in section 5.

1.1. The general dimer system

In the format of chemical reactions if we permit only monomer and dimer interactions, we include

$$C_2 + C_r \rightleftharpoons C_{r+2} \tag{6}$$

as well as (1). We define $\hat{a}_r$ ($\hat{b}_r$) to be the forward (reverse) reaction rate for the dimer interaction and also denote the net flux from cluster size r to $r+2$ to be K_r. The infinite set of differential equations to be studied are thus

$$\dot{c}_2 = J_1 - J_2 - K_2 - \sum_{r=1}^{\infty} K_r \tag{7}$$

$$\dot{c}_r = J_{r-1} - J_r + K_{r-2} - K_r \qquad r \geqslant 3 \tag{8}$$

$$J_r = a_r c_r c_1 - b_{r+1} c_{r+1} \qquad r \geqslant 1 \tag{9}$$

$$K_r = \hat{a}_r c_r c_2 - \hat{b}_{r+2} c_{r+2} \qquad r \geqslant 1 \tag{10}$$

where the choice of $\dot{c}_1$ produces two systems. If $\dot{c}_1 = 0$ then without loss of generality we assume $c_1 = 1$, alternatively to conserve the density, c_1 must vary according to

$$\dot{c}_1 = -J_1 - \sum_{r=1}^{\infty} J_r - K_1. \tag{11}$$

The additional complexity the dimer interaction introduces is evident in the equation for $\dot{c}_2$, (7), where the summation term couples the whole system together.

For an equilibrium solution we impose the condition that there must be no net flux of mass in the system, and we further insist upon a detailed balance condition so that each individual flux (9)–(10) is zero, so that the reactions (1) and (6) are balanced. With two interactions possible, we may construct a time-independent solution in which a local dimer aggregation, r to $r+2$, is balanced by a fragmentation flux of monomers ($K_r > 0$ with $J_r = J_{r+1} = -K_r$). However, if we remove all clusters of a particular size, $r+1$, then the equilibrium state will be disturbed, as the dimer interaction can no longer be balanced (since J_r is then positive). So while such a system satisfies a steady-state condition, we reject it as an equilibrium solution on the basis of detailed balancing which insists that the net flux of *each interaction* is zero, that is $J_r = 0$ and $K_r = 0, \forall r$. Considering the monomer fluxes to start with, we define a partition

function Q_r by $a_r Q_r = b_{r+1} Q_{r+1}$ together with $Q_1 = 1$, so that $J_r = 0$ is automatically satisfied. This yields the equilibrium solution

$$c_r = Q_r c_1^r. \tag{12}$$

Now we return to the dimer flux K_r and require that this equilibrium solution also satisfies $K_r = 0\ \forall r$. This yields an additional constraint on the forward and backward rate constants $\hat{a}$ and $\hat{b}$, namely,

$$\hat{a}_r = \hat{b}_{r+2} \left(\frac{b_2 a_r a_{r+1}}{a_1 b_{r+1} b_{r+2}} \right). \tag{13}$$

Hence, to define the four sets of rate coefficients (a, b, $\hat{a}$ and $\hat{b}$) we have only three degrees of freedom if the one equilibrium solution (12) is to satisfy the detailed balancing condition for both J_r and K_r fluxes.

While not being directly used in this paper we note that the following function is a Lyapunov function when fragmentation is stronger than aggregation:

$$V(c) = \sum_{r=1}^{\infty} c_r \left(\log \frac{c_r}{Q_r c_1^r} - 1 \right) \tag{14}$$

The asymptotic analysis used here does not rely on such a function existing. But we note that the existence of a Lyapunov function implies the uniqueness of the equilibrium solution and furthermore that the system is certain to tend to this equilibrium solution when V is bounded below. Since the Lyapunov function represents the free energy of the system, we use $V(c)$ to help interpret our results physically after the solution $\{c_r(t)\}_{t=1}^{\infty}$ has been determined.

2. Equilibrium state

2.1. Formulation

We now restrict ourselves to one particular example system. Until section 4 the monomer concentration is assumed to be constant; the obvious generalization is to allow this to vary. Additionally, we assume the aggregation and fragmentation rates are size-independent, namely $a_r = a$, $b_r = b$, $\hat{a}_r = \hat{a}$ and $\hat{b}_r = \hat{b}$. The consequence of assuming a constant monomer concentration is that the density of the system, ρ (5), will in general vary with time. To simplify much of the following analysis we define a parameter, θ, which indicates the relative strength of aggregation to fragmentation in the system:

$$\theta = \frac{a c_1}{b}. \tag{15}$$

Recalling from section 1.1 that to define the reaction rate coefficients we have only three degrees of freedom, we define a parameter k which reflects the relative strength of the dimer to the monomer interactions, and so,

$$\hat{a} = ka \qquad \hat{b} = kb. \tag{16}$$

2.2. Equilibrium solution

We may express the equilibrium solution in terms of θ as

$$c_r = \theta^{r-1} c_1. \tag{17}$$

A sensible boundary condition, on any solution, is to require that as $r \to \infty$, $c_r \to 0$, which for the above equilibrium configuration implies that $\theta < 1$. If $\theta \geqslant 1$ then we must look for a wider class of attractors, the steady-state solutions, which will be investigated in section 3. For the remainder of this section we assume $\theta < 1$.

2.3. Approach to equilibrium

Having found the equilibrium configuration we proceed further and calculate the manner in which this state is approached. We make the substitution $c_r(t) = c_r^{\text{equil}}\psi_r(t)$ so that the solution is separated into the time-independent final equilibrium solution, $c_r^{\text{equil}} = \theta^{r-1}c_1$, and a function which describes the dynamics by which this state is reached, $\psi_r(t)$. To be consistent with the boundary conditions mentioned earlier, ψ_r must satisfy

$$\begin{aligned} &\psi_r \to 1 \qquad \text{as} \quad r \to 1 \\ &\psi_r \to 0 \qquad \text{as} \quad r \to \infty. \end{aligned} \tag{18}$$

Substituting the above expression for $c_r(t)$ into $\dot{c}_r$ (8) yields

$$\frac{\partial \psi_r}{\partial t} = b\left[\psi_{r-1} - \psi_r - \theta\psi_r + \theta\psi_{r+1} + k\left(\psi_{r-2} - \psi_r - \theta^2\psi_r + \theta^2\psi_{r+2}\right)\right] \tag{19}$$

where we make the assumption that c_2 has reached its equilibrium value, namely $c_2 = \theta c_1$. This will be justified in the proceeding analysis as c_2 equilibrates faster than larger cluster sizes. Considering the large r region allows us to treat r as a continuous variable and so replace $\psi_r(t)$ by $\psi(r,t)$. Expanding the ψ terms in (19) using a Taylor expansion about the point (r,t), we obtain

$$\frac{\partial \psi}{\partial t} = b\left[\frac{\partial \psi}{\partial r}(-1 + \theta + 2k(\theta^2 - 1)) + \frac{1}{2}\frac{\partial^2 \psi}{\partial r^2}(1 + \theta + 4k(1 + \theta^2))\right] \tag{20}$$

where terms up to second order have been included.

Firstly we truncate this equation and only consider the first derivatives with respect to r and this gives a travelling wave solution $\psi = H(vt - r)$ with speed

$$v = b(1 - \theta)(1 + 2k + 2k\theta) \tag{21}$$

which is positive since θ is less than unity. To reveal the shape of the wave we must retain the second derivatives in equation (20) and transform the r coordinate to $z = r - vt - r_0$, to convert to a frame of reference in which the wave is stationary, where r_0 is a constant to be determined by matching to the solution at intermediate times. Denoting $\psi(r,t) = \bar{\psi}(z,t)$, we obtain

$$\frac{\partial \bar{\psi}}{\partial t} = \frac{b}{2}(1 + \theta + 4k(1 + \theta^2))\frac{\partial^2 \bar{\psi}}{\partial z^2} \tag{22}$$

which is subject to matching conditions $\bar{\psi} \to 1$ as $z \to -\infty$ and $\bar{\psi} \to 0$ as $z \to +\infty$. Subject to these conditions, equation (22) is satisfied by the self-similar solution $\bar{\psi} = \frac{1}{2}\text{erfc}\left(z\Big/\sqrt{2b(1 + \theta + 4k(1 + \theta^2))t}\right)$ and so

$$c_r(t) = \frac{1}{2}\theta^{r-1}c_1 \,\text{erfc}\left(\frac{r - tb[1 - \theta + 2k(1 - \theta^2)] - r_0}{\sqrt{2bt(1 + \theta + 4k[1 + \theta^2])}}\right). \tag{23}$$

Numerical simulations were performed using the Euler method to approximate the derivatives, a time step of 0.1 was found to be sufficient to produce reliable results. Double precision variables were used throughout and parameter values $a = 0.8$, $b = 1.2$ and $k = 0.5$ were chosen. The system was truncated at a maximum cluster size of 10^6, although we now believe this could be reduced significantly without affecting the results. In this case, with a phase shift of $r_0 = 6$, the analytical and numerical results were found to match to a high degree of accuracy.

2.4. Far-field asymptotics

Having previously calculated the form of the transition region, we proceed further and investigate the far-field region $r/s(t) > 1$, where $s(t) \sim vt$ is the position of the transition region as given by the centre of the wave (23). We postulate that the concentrations in the far-field region will be exponentially small and so apply a WKBJ asymptotic approximation $c_r(t) \sim \alpha(r,t)c_1\theta^{r-1}\,\mathrm{e}^{w(r,t)}$. Once again assuming r to be continuous we substitute this expansion into the definition (8) of $\dot{c}_r$. Expanding all terms to leading order we obtain

$$\frac{\partial w}{\partial t} = \frac{ac_1}{\theta}\,\mathrm{e}^{-\frac{\partial w}{\partial r}} - b - ac_1 + b\theta\,\mathrm{e}^{\frac{\partial w}{\partial r}} + \frac{kac_2}{\theta^2}\,\mathrm{e}^{-2\frac{\partial w}{\partial r}} - kb - kac_2 + kb\theta^2\,\mathrm{e}^{2\frac{\partial w}{\partial r}}. \tag{24}$$

We require w to take the self-similar form $w(r,t) = tF(\eta), \eta = r/t$, to match with the equation for ψ (23) in the transition region. Substitution of this form into the leading order WKBJ expansion yields

$$F(\eta) - \eta F'(\eta) = b\theta\,\mathrm{e}^{F'(\eta)} - b(1+k) - ac_1 - kac_2 + \frac{ac_1}{\theta}\,\mathrm{e}^{-F'(\eta)} + \frac{kac_2}{\theta^2}\,\mathrm{e}^{-2F'(\eta)} + kb\theta^2\,\mathrm{e}^{2F'(\eta)}. \tag{25}$$

We use the definition of θ (15) and the Legendre transform $F(\eta) \to \hat{F}(\hat{\eta}), \eta = \hat{F}'(\hat{\eta}), \hat{\eta} = F'(\eta)$ and $\eta\hat{\eta} = F(\eta) + \hat{F}(\eta)$ to obtain the solution

$$\hat{F}(\hat{\eta}) = -b\left[1 - \theta\,\mathrm{e}^{\hat{\eta}} + \theta - \mathrm{e}^{-\hat{\eta}} + k\left(1 - \frac{c_2}{\theta c_1}\,\mathrm{e}^{-2\hat{\eta}} + kac_2 - \theta^2\,\mathrm{e}^{2\hat{\eta}}\right)\right]. \tag{26}$$

Hence we may obtain the parametric solution by differentiating this expression to derive η and then substituting this result into $F(\eta) = \eta\hat{\eta} - \hat{F}(\hat{\eta})$. We assume that $c_2 = c_1\theta$ in the far-field region and hence obtain

$$\eta = -b(\theta\,\mathrm{e}^{\hat{\eta}} - \mathrm{e}^{-\hat{\eta}} - 2k\,\mathrm{e}^{-2\hat{\eta}} + 2k\theta^2\,\mathrm{e}^{2\hat{\eta}}) \tag{27}$$

$$F = -b\hat{\eta}(\theta\,\mathrm{e}^{\hat{\eta}} - \mathrm{e}^{-\hat{\eta}} - 2k\,\mathrm{e}^{-2\hat{\eta}} + 2k\theta^2\,\mathrm{e}^{2\hat{\eta}}) + b(\theta\,\mathrm{e}^{\hat{\eta}} - 1 - k - \theta - k\theta^2 + \mathrm{e}^{-\hat{\eta}} + k\,\mathrm{e}^{-2\hat{\eta}} + k\theta^2\,\mathrm{e}^{2\hat{\eta}}). \tag{28}$$

The first boundary condition this solution must satisfy is $F(\eta) \to -\infty$ as $\eta \to +\infty$ which corresponds to matching to the limit $r \to \infty$ where the concentrations tend to zero. If $\hat{\eta} \to -\infty$ then $\eta \to +\infty$, by inspection of equation (27), furthermore this implies that $F \to -\infty$ as required; hence the solution is consistent with this boundary condition. By considering the form of the WKBJ expansion $c_r(t) \sim \alpha(r,t)c_1\theta^{r-1}\,\mathrm{e}^{tF}$ we deduce that to match to the transition region we require $F = 0$ since if $F \neq 0$ the solution will tend to $\pm\infty$ as $t \to \infty$. We define η_c by $F(\eta_c) = 0$ and so this parameter will reveal the position of the transition region. Substituting $\hat{\eta} = 0$ into equation (28) gives $F = 0$ and hence we set $\hat{\eta} = 0$ in equation (27) to obtain

$$\eta_c = b(1-\theta)(1 + 2k + 2k\theta). \tag{29}$$

Since $\eta_c = r/t$ this expression is the velocity of the transition region and is in agreement with the previous analysis, namely, equation (21).

2.5. Lyapunov function

Differentiating $V(c)$ from (14) explicitly with respect to t and substituting for $\dot{c}_r$ from (7) and (8) we deduce that $V(c)$ monotonically decreases, but it is not clear that a lower limit exists.

Substituting an approximate solution $c_r = \theta^{r-1}H(vt - r)$, where H is the Heaviside step function, into (14) yields

$$V(c) = -\frac{1}{1-\theta} + \frac{\theta^{vt}}{1-\theta}. \tag{30}$$

Thus $V(c)$ has a lower bound and hence qualifies as a Lyapunov function, and V decreases exponentially to its equilibrium value, with a characteristic timescale of $\tau = 1/(v\ln\theta)$.

3. Steady-state solution

3.1. Formulation

We now consider the parameter regime where the equilibrium solution fails to be valid, namely, the case where $\theta > 1$. In this region, from previous work [5], we expect to find time-independent, or steady-state, solutions. The crucial difference between a steady-state and an equilibrium solution is that in the former we allow a net flux to flow through the system. Hence the equations to be solved are derived simply by setting $\dot{c}_r = 0\ \forall r$, in the definitions (7) and (8), this reduces to

$$0 = ac_1(c_2 - c_1) - b(c_3 - c_2) + kac_2^2 - kbc_4 + \sum_{r=1}^{\infty}(kac_2c_r - kbc_{r+2}) \tag{31}$$

$$0 = ac_1c_{r-1} - bc_r - ac_1c_r + bc_{r+1} + akc_2c_{r-2} - bkc_r - akc_2c_r + bkc_{r+2} \qquad r \geqslant 3. \tag{32}$$

We impose the conditions $c_r \geqslant 0$ and seek the weakest singularity in the limit as $r \to \infty$. Since (32) is a linear difference equation we assume $c_r = A\lambda^r$ and by substitution into (32), we derive a quartic equation for λ:

$$0 = (\lambda - 1)k\left[\lambda^3 + \lambda^2\left(\frac{1+k}{k}\right) + \lambda\left(-\frac{\theta}{k} - \frac{ac_2}{b}\right) - \frac{ac_2}{b}\right]. \tag{33}$$

The four roots are easily determined in the limiting cases $k \ll 1$ and $k \gg 1$. For $k \ll 1$ we find $\lambda_1 = \theta$, $\lambda_2 = -1/k$, $\lambda_3 = -akc_2/(\theta b)$ and $\lambda_4 = 1$. Assuming $k \gg 1$ yields $\lambda_1 = \sqrt{ac_2/b}$, $\lambda_2 = -1$, $\lambda_3 = -\sqrt{ac_2/b}$ and $\lambda_4 = 1$. Explicitly plotting the roots, from the quartic equation, over a wide range of parameters θ and k has shown that the roots are limited to the ranges $1 < \lambda_1,\ \lambda_2 < -1$, $-1 < \lambda_3 < 0$ and $\lambda_4 = 1$. Clearly the physical conditions, $c_r \geqslant 0$ and $c_r \not\to +\infty$ as $r \to \infty$, require that $|\lambda| \leqslant 1$ and thus eliminate λ_1 and λ_2 as possibilities, henceforth we denote λ_3 as simply λ. So the 'weakest singularity' condition implies keeping λ_3 and λ_4 to obtain the solution $c_r = A + B\lambda^{r-1}$; however, we note that such a solution cannot satisfy (31). As the following calculations will confirm, it is necessary to include an additional term to reflect the influence of the next-order terms and so we make the ansatz

$$c_r^{sss} = A + B\lambda^{r-1} + \frac{\chi_r}{t}. \tag{34}$$

We substitute this ansatz into equation (32), and take the large-time limit; the leading-order solution will be zero by the definition of λ. At $O(1/t)$ we obtain the recurrence relation

$$\begin{aligned} ac_1\chi_{r-1} - b\chi_r - ac_1\chi_r + b\chi_{r+1} + ak(A + B\lambda)\chi_{r-2} bk\chi_r - ak(A + B\lambda)\chi_r + bk\chi_{r+2} \\ = ka\chi_2(A + B\lambda^{r-1}) - ka\chi_2(A + B\lambda^{r-3}) \end{aligned} \tag{35}$$

for χ_r. The complementary function of this equation satisfies the condition on c_r (32), where $A + B\lambda = c_2$. This allows the reuse of previous analysis; indeed χ_r is subject to similar physical conditions as c_r, namely $\chi_r \not\to +\infty$ as $r \to \infty$. Thus we obtain

$$\chi_r = Pr\lambda_r + Q\lambda^r + R \tag{36}$$

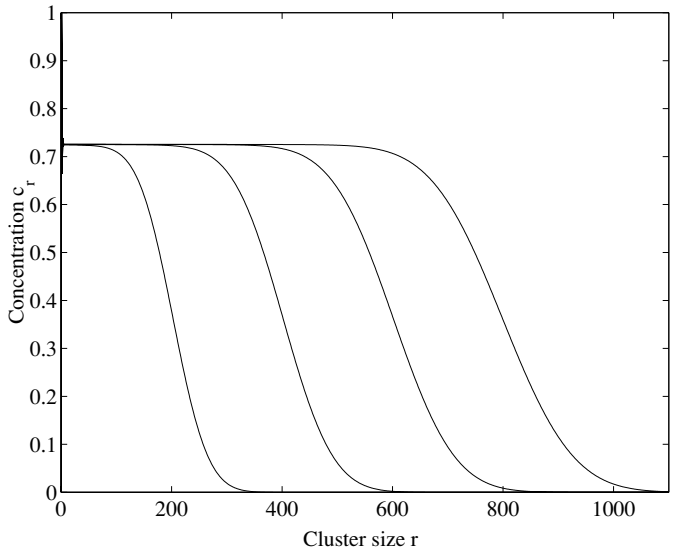

Figure 1. A plot of the concentration profile of the clusters at times 500, 1000, 1500, 2000, centred at $r = 200$, 400, 600 and 800, respectively, for the system parameters $a = 1.2$, $b = 0.8$ and $k = 0.5$ for the constant monomer case. Note the broadening of the wave at later times.

with P, Q and R as constants where $Pr\lambda^r$ is the particular solution of (35). Substitution of this into the difference equation (35) results in an expression connecting P and χ_2

$$P = \frac{k\chi_2(b-a)(\lambda+1)}{2kb\lambda^5 + b\lambda^4 - ac_1\lambda^2 - 2bk\lambda}. \tag{37}$$

Furthermore, we impose the condition that $\chi_1 = 0$, since $c_1 = 1$ is a given constant, and so deduce that $R = -P\lambda - Q\lambda$. Substituting $r = 2$ into the general solution (36), together with the expression for R, reveals that

$$Q = \frac{\chi_2 - P(2\lambda^2 - \lambda)}{\lambda^2 - \lambda}. \tag{38}$$

So only χ_2 remains undetermined in (36); this can be determined only when the full form of the large-time asymptotical solution is known.

3.2. First-order correction theory

To gain an insight into the following calculation it is instructive to study the results of a numerical simulation. Once again an Euler method was used but with $a = 1.2$, $b = 0.8$ and $k = 0.5$, a time step of 0.001 was required to produce reliable results, that is halving this time step did not affect the results. This system was truncated at cluster size 2000, with particles able to aggregate out of the system; that is the fragmentation rates b_{2001} and b_{2002} were assumed to be zero. The concentration profile at times 500, 1000, 1500 and 2000 has been plotted in figure 1. As in the $\theta < 1$ case we split the system into three regions: (i) the lower sized clusters, which have reached their steady-state concentrations, (ii) cluster sizes in the transition region and (iii) larger cluster sizes whose concentrations are still zero. The numerical simulations strongly suggest the following relationship for the position of the transition region, $r = s(t)$, and for the concentration of $c_2(t)$ in the large-time limit:

$$s(t) = (ac_1 - b)t \tag{39}$$

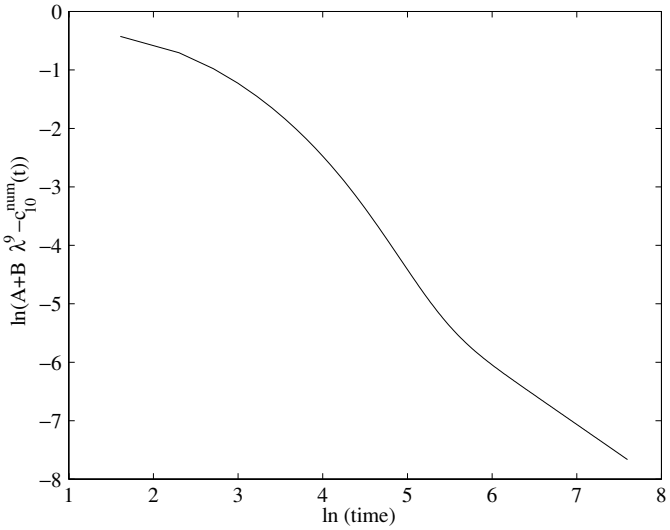

Figure 2. A plot of $\log(A + B\lambda^9 - c_{10}^{\mathrm{num}}(t))$ against $\log(t)$ for the constant monomer case with $a = 1.2$, $b = 0.8$ and $k = 0.5$. The gradient between times $\log t = 1495$ and $\log t = 1995$ was found to be -1.003, confirming a $1/t$ form for the first correction term.

$$c_2 = \frac{b}{a} \qquad \text{as} \quad t \to \infty \tag{40}$$

the validity of these relationships will be justified in the following analysis. The combination of (40) and $c_1 = 1$ in the limit $t \to \infty$ implies

$$A = \frac{\lambda - \frac{b}{a}}{\lambda - 1} \qquad \text{and} \qquad B = \frac{\frac{b}{a} - 1}{\lambda - 1}. \tag{41}$$

We are now able to test the ansatz (34) for $c_r(t)$ directly against the numerics. By plotting $A + B\lambda^9 - c_{10}^{\mathrm{num}}(t)$, where $c_r^{\mathrm{num}}(t)$ is the numerical concentration of cluster size r at time t, we extract the first correction term which should equal χ_{10}/t. In figure 2 the logarithm of the correction term is plotted against $\log(t)$ giving a gradient of -1.003 between times 1495 and 1995. This gives excellent agreement with the χ_r/t form of (34).

The standard first-order continuum approach approximates the system by $c_r(t) = c_r^{sss} H(s(t) - r)$, where H is the Heaviside step function located at $r = s(t)$. In this case we have $c_r^{sss} = A + B\lambda^r$ for $r < s(t)$ and $c_r = 0$ otherwise and obtain an expression for the density by combining this approximation with the definition (5). For large r, $c_r^{sss} \sim A$ so $\rho \sim s^2 A/2$ and differentiating gives $\dot{\rho} \sim c_\infty s\dot{s}$. Another method of obtaining $\dot{\rho}$ is to differentiate (5) directly, leading to

$$\dot{\rho} = J_1 + \sum_{r=1}^{\infty} J_r + K_1 \tag{42}$$

by substitution for $\dot{c}_r$ from equations (7) and (8). Using the approximation that only two regions are present, separated at $s(t)$, this expression reduces to $\dot{\rho} \sim As(ac_1 - b)$. By comparing the two equations for $\dot{\rho}$ we obtain $s(t) \sim (ac_1 - b)t$, thus confirming the result assumed above. While this approach has successfully predicted the location of the transition region it does not account for any sensitive behaviour there. To highlight a weakness of the first-order continuum theory K_r has been plotted at times 500, 1000, 1500 and 2000 in figure 3,

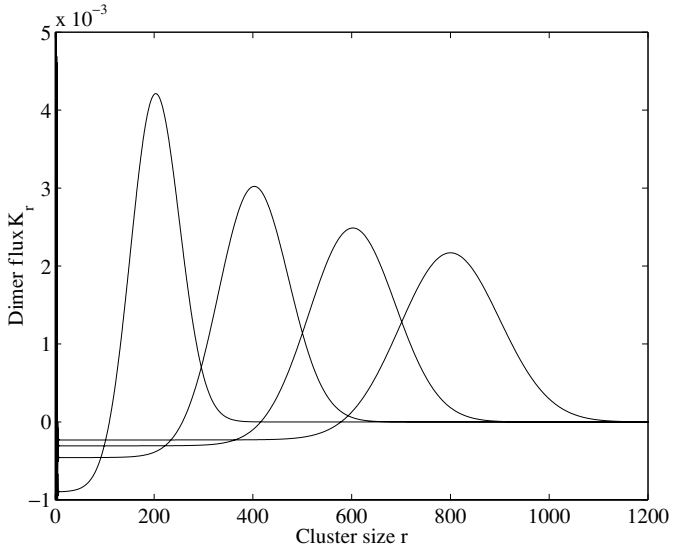

Figure 3. A plot of the profile of values of $K_r(t)$ at times 500, 1000, 1500, 2000 with $a = 1.2$, $b = 0.8$ and $k = 0.5$ for the constant monomer case. The peak of each curve is centred on the transition region ($r = s(t)$).

where the peak is centred on the transition region. From this figure it is clear that the form of the transition region is important as this produces a large peak in the K_r profile which otherwise would not be taken into account. However, in the preceding analysis only K_1 was required and so the simplified approach correctly predicts the speed of the transition region, but to proceed with a more detailed analysis we must first determine its shape.

3.3. Second-order continuum theory

The approach employed in section 2.3 for the $\theta < 1$ case can be used to determine how the system approaches the steady-state solution. Using (34) and (36) we decompose the solution into $c_r(t) = c_r^{sss}\psi_r(t)$ where

$$c_r^{sss} = A + B\lambda^{r-1} + \frac{Pr\lambda^r}{t} + \frac{Q\lambda^r}{t} + \frac{R}{t}. \tag{43}$$

We substitute the decomposition of $c_r(t)$ into (8), assume a continuum approximation for r, and expand all terms about the point (r, t) and retain only the first two correction terms. Furthermore as in section 2.3, the coordinates are transformed by $z = r - s(t)$ and $\psi(r, t) = \bar{\psi}(z, t)$, to focus on the transition region. Taking the large time limit, in which we note that $\lambda^{s(t)} \to 0$ as $|\lambda| < 1$, the leading order equation becomes

$$\frac{\partial\bar{\psi}}{\partial t} - \dot{s}\frac{\partial\bar{\psi}}{\partial z} = (b - ac_1)\frac{\partial\bar{\psi}}{\partial z} + \frac{1}{2}(b + ac_1 + 8kb)\frac{\partial^2\bar{\psi}}{\partial z^2}. \tag{44}$$

The $\frac{\partial\bar{\psi}}{\partial z}$ terms cancel, as in this frame of reference the transition region is stationary, again confirming (39). The remaining terms have the same form as (22) and so produce the solution

$$\psi(r, t) = \frac{1}{2}\mathrm{erfc}\left(\frac{r - t(ac_1 - b)}{\sqrt{2b(\theta + 1 + 8k)t}}\right). \tag{45}$$

To test this result we have plotted, in figure 4, $c_r(t) = c_r^{sss}\psi(r, t)$ against r alongside the numerical values of $c_r(t)$ at time $t = 1000$; clearly the difference is small, lending weight to

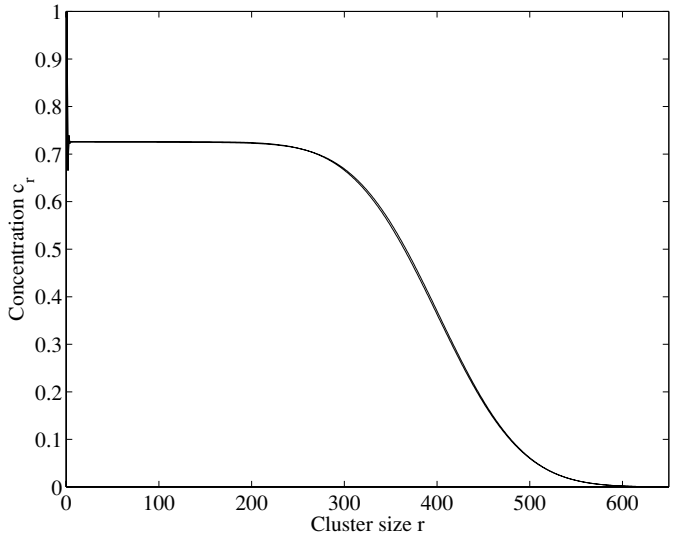

Figure 4. The steady-state solution, c_r^{sss}, and the numerical values for $c_r(t)$ plotted for a range of r at time 1000 with $a = 1.2$, $b = 0.8$ and $k = 0.5$ for the constant monomer case. The two cases are almost indistinguishable.

the analysis; furthermore the discrepancy tends to zero in the large time limit. In summary we now have the form of the solution in the large-time asymptotic domain, namely,

$$c_r(t) = \frac{1}{2}\left(A + B\lambda^{r-1} + \frac{Pr\lambda^r}{t} + \frac{Q\lambda^r}{t} + \frac{R}{t}\right)\operatorname{erfc}\left(\frac{r - t(ac_1 - b)}{\sqrt{2b(\theta + 1 + 8k)t}}\right) \tag{46}$$

as $t \to \infty$ with $r - (ac_1 - b)t = O\left(t^{\frac{1}{2}}\right)$. However, P, Q and R depend on χ_2 which is as yet unknown, also we have yet to show that the dimer equation (31) is satisfied by this solution.

Before we can assess the consistency of (31) we must focus on evaluating the sum $\sum_{r=1}^{\infty} K_r$ using (46); the form of c_{r+2} can be obtained from (46)

$$c_{r+2} = \frac{1}{2}\left(A + B\lambda^{r+1} + \frac{P}{t}((r+2)\lambda^{r+2}) + \frac{Q}{t}(\lambda^{r+2}) + \frac{R}{t}\right)\operatorname{erfc}\left(\frac{r - (ac_1 - b)t}{\sqrt{\beta t}} + \frac{2}{\sqrt{\beta t}}\right) \tag{47}$$

where for simplicity we denote $\beta = 2b(\theta + 1 + 8k)$. Expanding the erfc function using a Taylor series about the point $r - (ac_1 - b)t/\sqrt{\beta t}$, we obtain from (10)

$$\begin{aligned} K_r = kb\Bigg[B\lambda^r\left(\frac{1}{\lambda} - \lambda\right) + \frac{P}{t}(r\lambda^r - (r+2)\lambda^{r+2}) + \frac{Q}{t}(\lambda^r - \lambda^{r+2})\frac{a\chi_2}{bt}\left(A + B\lambda^{r-1}\right. \\ \left. + \frac{P}{t}(r\lambda^r - \lambda) + \frac{Q}{t}(\lambda^r - \lambda)\right)\Bigg]\operatorname{erfc}\left(\frac{r - (ac_1 - b)t}{\sqrt{\beta t}}\right) + \Bigg[A + B\lambda^{r+1} \\ + \frac{P}{t}((r+2)\lambda^{r+2}) + \frac{Q}{t}(\lambda^{r+2}) + \frac{R}{t}\Bigg]\frac{2kb}{\sqrt{\beta\pi t}}\exp\left(-\left(\frac{r - (ac_1 - b)t}{\sqrt{\beta t}}\right)^2\right). \end{aligned} \tag{48}$$

Returning to (31), we now consider the summation of this expression from $r = 1$ to ∞, which we can split into two terms. Since the speed of the outgoing wave is proportional to t, whereas the width of the wave is proportional to $\sqrt{t}$, the erfc function in the first term is well

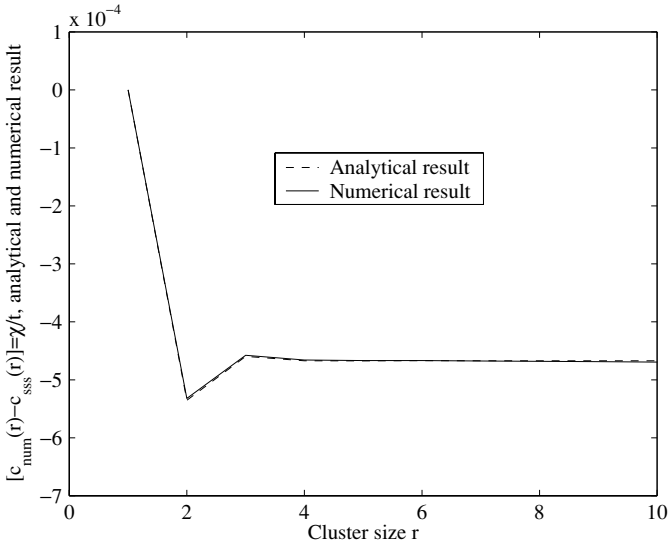

Figure 5. The correction term $\chi_r = Pr\lambda^r + Q\lambda^r + R$ from asymptotic analysis and $c_r^{\text{num}} - (A + B\lambda^{r-1})$, the numerical value, are plotted against r, in the constant monomer case with $a = 1.2$, $b = 0.8$ and $k = 0.5$. A favourable comparison supports the analytical approach taken.

approximated by a step function located at $s(t)$, in the large time limit, and so the sum of this term may be confined $r = 1$ to $s(t)$ and the erfc function eliminated. To leading order this provides a contribution of $kB(1 + \lambda) + ka\chi_2 A(ac_1 - b)$ to $\sum_{r=1}^{\infty} K_r$. Turning to the latter term in equation (48), since we are in the large time limit this places the Gaussian at a large value of r, implying that terms of $r = O(1)$ will be exponentially small, and allows us to take the large r limit of the pre-multiplying factor. Additionally, by virtue of the fact that the Gaussian is located at large r, we can approximate the sum by an integral and extend the limits to $\pm\infty$ as the contributions due to $r < 1$ will be exponentially small. Performing all the above calculations yields a contribution of $2kbA$. Combining the two contributions, we finally obtain

$$\sum_{r=1}^{\infty} K_r = kB(1 + \lambda) + ka\chi_2 A(ac_1 - b) + 2kbA. \tag{49}$$

The significance of retaining the first correction term in the expansion for c_r is the addition of $2kbA$, from the latter term in equation (48), which cannot be found from a first-order continuum theory.

Substituting the expression (49) into (31) gives

$$\chi_2 = \frac{c_1(ac_1 - b) - \frac{b^2}{a}(1 + k) + bA(1 - k) + bB(k\lambda^3 + \lambda^2 - k\lambda - k)}{Aka(ac_1 - b)} \tag{50}$$

since to leading order $J_1 = ac_1^2 - b^2/a$, $J_2 = bc_1 - b(A + B\lambda^2)$ and $K_2 = kb^2/a - kb(A + B\lambda^3)$ and P, Q, R are known constants given by (37) and (38); hence χ_r is fully defined by (36).

We directly compare the analytical result for χ_r with $c_r^{\text{num}} - (A + B\lambda^{r-1})$, which is the numerical value of the correction term, for small cluster sizes at time $t = 1995$. The parameter values used were $a = 1.2$, $b = 0.8$, $k = 0.5$ and a time step of 0.001 with initial conditions $c_1 = 1$, $c_r = 0$ for $r \geqslant 2$. Figure 5 shows the comparison and the agreement is good.

3.4. Far-field asymptotics

The far-field analysis of the steady-state solution is similar to that presented in section 2.4. Since at large r we have $c_r = A$, in this case the WKBJ approximation is $c_r(t) \sim A\alpha(r,t)\exp(w(r,t))$. The omission of $\theta^{r-1}c_1$ in the expansion transforms (24) into

$$\frac{\partial w}{\partial t} = ac_1\,\mathrm{e}^{-\frac{\partial w}{\partial r}} - b - ac_1 + b\,\mathrm{e}^{\frac{\partial w}{\partial r}} + kac_2\,\mathrm{e}^{-2\frac{\partial w}{\partial r}} - kb - kac_2 + kb\,\mathrm{e}^{2\frac{\partial w}{\partial r}} \tag{51}$$

and, following (25), we substitute $w(r,t) = tF(\eta)$ with $\eta = r/t$ to obtain

$$F(\eta) - \eta F'(\eta) = b\,\mathrm{e}^{F'(\eta)} - b(1+k) - ac_1 - kac_2 + ac_1\,\mathrm{e}^{-F'(\eta)} + kac_2\,\mathrm{e}^{-2F'(\eta)} + kb\,\mathrm{e}^{2F'(\eta)}. \tag{52}$$

As before, we apply the Legendre transform $F(\eta) \to \hat{F}(\hat{\eta})$, $\eta = \hat{F}'(\hat{\eta})$, $\hat{\eta} = F'(\eta)$ and $\eta\hat{\eta} = F(\eta) + \hat{F}(\eta)$ to equation (52) and assume that $c_2 = b/a$, the equilibrium value, to obtain

$$\hat{F} = b(1 + 2k + \theta - \mathrm{e}^{\hat{\eta}} - \theta\,\mathrm{e}^{-\hat{\eta}} - k\,\mathrm{e}^{-2\hat{\eta}} - k\,\mathrm{e}^{2\hat{\eta}}) \tag{53}$$

$$\eta = b(\theta\,\mathrm{e}^{-\hat{\eta}} - \mathrm{e}^{\hat{\eta}} + 2k\,\mathrm{e}^{-2\hat{\eta}} - 2k\,\mathrm{e}^{2\hat{\eta}}). \tag{54}$$

As $\hat{\eta} \to -\infty$, from equation (54), we see that $\eta \to +\infty$ and also $F \to -\infty$ from equation (53); hence the solution satisfies the boundary condition $c_r(t) \to 0$ as $r \to +\infty$. The edge of the transition region is given by η_c, defined by $F(\eta_c) = 0$, which implies $\hat{\eta} = 0$ in equations (53) and (54) and so

$$\eta_c = b(\theta - 1). \tag{55}$$

Since $\eta = r/t$, equation (55) reveals that the position of the transition region $s(t) = (ac_1 - b)t$, which confirms the earlier analysis.

3.5. Lyapunov function

For the case $\theta < 1$ we found that $V(c)$ was a Lyapunov function, ensuring the system approached the equilibrium solution and here we once again investigate the behaviour of this function. The complementary error function in $c_r(t)$ is approximated by a Heaviside step function, $H(x)$, to give

$$c_r \approx \left[A + B\lambda^{r-1} + \frac{P}{t}(r\lambda^r - \lambda) + \frac{Q}{t}(\lambda^r - \lambda)\right] H(s(t) - r). \tag{56}$$

By inspection we see that $c_r \to A$ for $1 \ll r < s$ as $t \to \infty$ and so with the definition of $V(c)$ as given in (14), we obtain

$$V(c) \approx \sum_{r=1}^{s} \left(\log\left(\frac{A}{Q_r c_1^r}\right) - 1\right) c_r. \tag{57}$$

As $s \to \infty$ the argument of the logarithm tends to zero from above, so that the logarithm tends to $-\infty$. Since the summation incorporates increasingly large negative values, it too must tend to $-\infty$ implying the non-existence of a lower bound. So although the function V is well defined in (14), it fails to qualify as a Lyapunov function since it is not bounded below.

4. Constant density systems

4.1. Formulation

In this section we study the modified Becker–Döring equation similar to that proposed by Penrose [2], in that the density ρ is held constant and the monomer concentration is allowed to vary, but we further allow dimers to interact. The system has the form

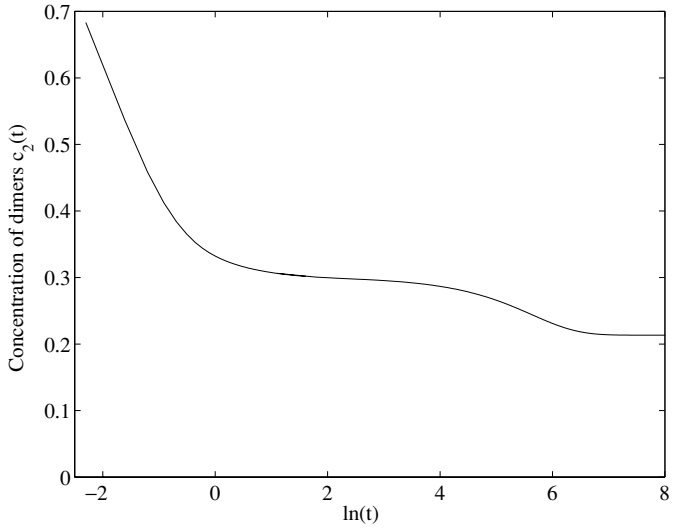

Figure 6. In the constant mass formulation of the Becker–Döring system, a strong dimer interaction leads to two timescales in the problem. This is illustrated by the behaviour of c_2, as plotted against $\log(t)$ with $a = 0.0024$, $b = 0.0016$ and $k = 1000$ with an initial state of $c_2 = 1$ and all other concentrations being zero. Clearly, after a fast phase the system remains in a pseudo-equilibrium until finally a slower phase forces the system to its final equilibrium state.

$$\dot{c}_1 = -J_1 - \sum_{r=1}^{\infty} J_r - K_1 \tag{58}$$

$$\dot{c}_2 = J_1 - J_2 - K_2 - \sum_{r=1}^{\infty} K_r \tag{59}$$

$$\dot{c}_r = J_{r-1} - J_r + K_{r-2} - K_r \qquad r \geqslant 3 \tag{60}$$

where J_r and K_r are defined previously, (9) and (10). To make analytical progress we take the fragmentation and aggregation coefficients $a_r, b_r, \hat{a}_r$ and $\hat{b}_r$ to be independent of cluster size, that is $\hat{a}_r = \hat{a}, a_r = a, b_r = b$ and $\hat{b}_r = \hat{b}$. Once again the detailed balanced condition requires that $\hat{a} = ka$ and $\hat{b} = kb$. We will investigate the case of a strong dimer interaction, by assuming $k \gg 1$, which causes all even-sized clusters to rapidly evolve to a local equilibrium, and similarly for odd-sized clusters, after which the system slowly tends towards a global equilibrium. To highlight the diverse timescales we assume that only dimer clusters are present initially, that is $c_1 = 0, c_2 = 1$ and $c_r = 0$ for $r \geqslant 2$. To illustrate the two timescales embedded in the problem, we performed a numerical simulation similar to that outlined in section 3.1. Parameter values of $a = 0.0024, b = 0.0016, k = 1000$ and a time step of 0.001 were used and, in figure 6, c_2 is plotted against $\log(t)$ showing the widely differing timescales present. After an initial fast phase, over which the system separately equilibrates the even-sized clusters and the odd-sized clusters, there follows an equilibration over a much longer timescale, as can be seen by the second drop in c_2.

To investigate these timescales we systematically derive those variables which are unaffected by the dimer interaction, by analysing the rate of change of a quantity G given by $G = \sum_{r=1}^{\infty} g_r c_r$. This uses the weak form

$$\sum_{r=1}^{\infty} g_r \dot{c}_r = \sum_{r=1}^{\infty} (g_{r+1} - g_r - g_1) J_r + \sum_{r=1}^{\infty} (g_{r+2} - g_r - g_2) K_r \tag{61}$$

a similar result for the standard Becker–Döring equations was used by Ball *et al* [3] in a highly detailed analysis of that system. By considering equation (61) we deduce that those variables which are unaffected by the dimer flux must satisfy the recurrence relation $g_{r+2} = g_r + g_2$, which has the solution

$$g_r = \tfrac{1}{2} r g_2 + \left(\tfrac{1}{2} g_1 - \tfrac{1}{4} g_2\right)\left(1 - (-1)^r\right) \tag{62}$$

and defining g_1 and g_2 will select a solution. If $g_1 = 1$ and $g_2 = 2$ then we recover the density (5) from (62), namely $G = \rho$, which is a constant of motion ($\dot{\rho} = 0$). However, if $g_1 = 1$ and $g_2 = 0$ then we obtain $G = N_o$, whence we define a new variable $N_o(t)$ to be the number of clusters consisting of odd numbers of monomers

$$N_o = \sum_{r=1}^{\infty} c_{2r-1}. \tag{63}$$

So N_o is the only other variable not to depend on the dimer flux and hence will be a constant over the fast timescale, which is governed solely by the dimer interaction, but will vary on the slow timescale. We make use of these features of N_o to investigate the separate timescales.

4.2. Fast timescale

Over the fast timescale we make the simplifying assumption that there are no monomer interactions as the dynamics proceeds solely by the dimer interactions. We therefore postulate that $a = b = 0$, and hence all the J_r fluxes are zero, whilst retaining non-zero $\hat{a}$ and $\hat{b}$; therefore

$$\dot{c}_1 = -K_1 \tag{64}$$

$$\dot{c}_2 = -K_2 - \sum_{r=1}^{\infty} K_r \tag{65}$$

$$\dot{c}_r = K_{r-2} - K_r. \tag{66}$$

While it is not possible to solve these equations for all t, it is possible to calculate the pseudo-equilibrium state that the system relaxes to on the fast timescale. When the dimer interactions have equilibrated the pseudo-equilibrium solution has the form

$$c_{r+2} = \left(\frac{\hat{a}}{\hat{b}} c_2\right) c_r = \hat{\theta}^2 c_r \tag{67}$$

where $\hat{\theta} = \sqrt{\hat{a} c_2 / \hat{b}}$; we note that this variable is time-dependent. This relation reduces the problem to a two-dimensional system and so we denote the pseudo-equilibrium state in terms of two parameters, c_1 and c_2,

$$c_{2r} = c_2 \hat{\theta}^{2r-2} \qquad c_{2r+1} = c_1 \hat{\theta}^{2r}. \tag{68}$$

From equations (63), (64) and (66) we deduce $\dot{N}_o = 0$, that is N_o is a constant of motion as predicted by the analysis in section 4.1. Using the expressions for the equilibrium solution (68) and the definition of N_o (63), we further derive

$$N_o = c_1 \left(\frac{1}{1 - \hat{\theta}^2}\right). \tag{69}$$

Performing a similar calculation for the other constant of motion, ρ defined in equation (5), reveals that

$$\rho = \frac{1}{(1 - \hat{\theta}^2)^2}\left(2c_2 + c_1(1 + \hat{\theta}^2)\right). \tag{70}$$

Eliminating c_2 from this equation, by using $\hat{\theta}$, and then combining the result with equation (69) gives an expression for $\hat{\theta}$ solely in terms of known constants of motion

$$\hat{\theta}^2 = \frac{(2\rho + 2\hat{b}/\hat{a}) \pm \sqrt{4\hat{b}^2/\hat{a}^2 + 8\rho\hat{b}/\hat{a} + 4N_o^2}}{2(\rho + N_o)}. \tag{71}$$

Hence the pseudo-equilibrium state is fully defined, as described for a particular case below. Using the values for $\hat{a}$, $\hat{b}$ and ρ from figure 6, namely, $\hat{a} = 0.0024$, $\hat{b} = 0.0016$ and $\rho = 2$, (71) yields $\hat{\theta}^2 = 0.4514$ where we have rejected the solution which predicts a larger density than exists in the system. Utilizing $c_2 = \hat{\theta}^2\hat{b}/\hat{a}$ we obtain $c_2 = 0.3009$, the pseudo-equilibrium concentration after the fast phase but prior to the slow phase, and this value is in agreement with the data in figure 6. At the end of the fast phase, the odd-sized clusters remain at effectively zero concentrations ($c_{2r+1} = O(1/k)\ \forall r$) whilst the even-sized clusters are given by (68). With knowledge of c_2 and $\hat{\theta}^2$ the pseudo-equilibrium concentration of any cluster size is revealed by exploiting equations (68) and (69).

Continuing with the numerical example given above we interpret the two timescales physically via the Lyapunov function, which represents a free energy of the system. We calculate the Lyapunov function at three times, initially (at $t = 0$, where $V = V_0$), at the end of the fast phase (where $t = O(1/k)$ and $V = V_f$) and at equilibrium, which occurs at the end of the slow phase (on a timescale of $t = O(1)$; as $t \to \infty$ $V \to V_\infty$), and find that

$$V_0 = -1.405 \qquad V_f = -2.154 \qquad V_\infty = -2.819. \tag{72}$$

Since the absolute size of the drop over the fast and slow phases is of the same order of magnitude, we deduce that both timescales represent equally important processes; however, the rate of change of free energy ($\dot{V}$) will be much greater in the first timescale than the latter.

4.3. Slow timescale

Having identified a slow timescale over which the system finally reaches a global equilibrium, we now proceed to make some assumptions valid in this region and aim to evaluate the relaxation time. The large dimer interaction will ensure that upon reaching the slow timescale, the K_r terms will all be zero. This provides a connection between all the even-sized clusters, and similarly the odd-sized clusters, in the following manner:

$$c_{2r} = \left(\frac{ac_2}{b}\right)^{r-1} c_2 \qquad c_{2r-1} = \left(\frac{ac_2}{b}\right)^{r-1} c_1. \tag{73}$$

To calculate the slow timescale, we linearize around the global equilibrium solution by $c_1(t) = \bar{c}_1 + \chi_1(t)$ and $c_2(t) = \bar{c}_2 + \chi_2(t)$, where $\bar{c}_1$ and $\bar{c}_2$ are the equilibrium values of c_1 and c_2, respectively. Investigating how the functions $\chi_1(t)$ and $\chi_2(t)$ decay to zero reveals the appropriate timescale.

Equations (73) reduce the system from an infinite array to a two-dimensional system. By substituting the expressions (73) into (5), we obtain

$$c_1 = \frac{\rho(b - ac_2)^2 - 2b^2c_2}{b(b + ac_2)} \tag{74}$$

and so using the linearization $c_1 = \bar{c}_1 + \chi_1$ and $c_2 = \bar{c}_1 + \chi_2$ in this equation, assuming $\chi_1 \ll \bar{c}_1$ and $\chi_2 \ll \bar{c}_2$, we gain an expression linking χ_1 and χ_2, namely

$$\chi_1 = \left(\frac{2a^2\rho\bar{c}_2 - 2ab\rho - 2b^2 - ab\bar{c}_1}{b^2 + ab\bar{c}_2}\right)\chi_2. \tag{75}$$

Recalling from section 4.1 that N_o is the only variable to be unaffected by the fast phase, we shall make use of it to calculate an estimate of the slow timescale. It is possible to evaluate

$\dot{N}_o$ in two ways and equating these gives an expression for $\dot{c}_2$. Firstly we evaluate N_o directly from the definition (63), equations (73) and (74) to give

$$N_o = \frac{\rho(b - ac_2)^2 - 2b^2c_2}{(b - ac_2)^2}. \tag{76}$$

Differentiating this with respect to time gives

$$\dot{N}_o = \left(\frac{-2b^2(b + ac_1 + ac_2)}{(b + ac_2)(b - ac_2)^2}\right)\dot{c}_2. \tag{77}$$

Alternatively, we use $\dot{N}_o = -2\sum_{r=1}^{\infty} J_{2r-1}$ and the definition of J_r in (9) to obtain $\dot{N}_o = 2b\left(bc_2 - ac_1^2\right)\big/(b - ac_2)$; equating this with equation (77) gives

$$\dot{c}_2 = \frac{\left(ac_1^2 - bc_2\right)(b + ac_2)(b - ac_2)}{b(b + ac_1 + ac_2)}. \tag{78}$$

Finally, using $c_1 = \bar{c}_1 + \chi_1$ and $c_2 = \bar{c}_2 + \chi_2$ in this equation, and using equation (75) to eliminate χ_1 implies $\dot{\chi}_2 = -\chi_2/\tau$, where

$$\tau = \frac{b^2(b + a\bar{c}_1 + a\bar{c}_2)}{(a\bar{c}_2 - b)\left(4a^3\rho\bar{c}_1\bar{c}_2 - 4a^2b\rho\bar{c}_1 - 4ab^2\bar{c}_1 - 2a^2b\bar{c}_1^2 - b^3 - ab^2\bar{c}_2\right)} \tag{79}$$

and so the slow timescale is τ.

To compare this result with the numerical simulations, as detailed in section 3.1, we calculate the gradient of $\log\left(c_2^{\text{num}} - \bar{c}_2\right)$ against t, where c_2^{num} is the value of c_2 from a numerical simulation, which will equal $1/\tau$ if the analysis is valid. Fixing $\rho = 2$ and $a = 0.002$ we compared this gradient for a range of b values and the results were found to match to a high degree of accuracy.

4.4. Arbitrary rate coefficients

For the constant density case with arbitrary rate coefficients, a similar evolution is observed, namely a fast phase where the even-sized clusters self-equilibrate and the odd-sized clusters self-equilibrate, but the even- and odd-sized clusters are not in equilibrium with each other. Following a meta-stable timescale, there follows a slower phase of kinetics during which the even- and odd-sized clusters reach a global equilibrium solution.

As described above, the only quantities which do not alter on the fast phase are the total density, which does not vary over the slow timescale either, and the number of odd-sized clusters, $N_o(t)$. Thus at the end of the fast phase of aggregation and fragmentation, $N_o(t) = N_o(0)$. Over the fast phase, the kinetics are governed by (64)–(66). In the slow phase of the process, all the dimer fluxes K_r are always zero, and so the kinetics are formally governed by the normal Becker–Döring equations (3)–(5).

However, the conditions that $K_r = 0$ constitute recurrence relations which relate all the even-sized clusters to c_2 and all the odd-sized clusters to some combination of c_2 and c_1. Solving these recurrence relations yields a reduction of the full system of equations for $\{c_r(t)\}_{r=1}^{\infty}$ to a two-dimensional system for $\{c_1(t), c_2(t)\}$ by way of

$$c_r^{\text{even}}(t) = Q_r\left(\sqrt{\frac{b_2c_2(t)}{a_1}}\right)^r \qquad c_r^{\text{odd}}(t) = Q_r\left(\sqrt{\frac{b_2c_2(t)}{a_1}}\right)^{r-1} c_1(t). \tag{80}$$

The two equations which are then used to determine the evolution of c_1, c_2 are (i) conservation of density

$$\varrho = \sum_{k=1}^{\infty} 2kQ_{2k}\left(\frac{b_2c_2(t)}{a_1}\right)^k + (2k-1)Q_{2k-1}\left(\frac{b_2c_2(t)}{a_1}\right)^{k-1} c_1(t) \tag{81}$$

and (ii) the evolution of $N_o(t)$, which satisfies

$$\dot{N}_o = -2\sum_{k=1}^{\infty} J_{2k-1}. \tag{82}$$

During the slow phase, the monomer concentration is given by

$$c_1(t) = \frac{\varrho - \sum_{k=1}^{\infty} 2kQ_{2k}(b_2c_2(t)/a_1)^k}{\sum_{k=1}^{\infty}(2k-1)Q_{2k-1}(b_2c_2(t)/a_1)^{k-1}} \tag{83}$$

which enables the kinetics to be written in terms of a first-order ordinary differential equation. This is obtained by calculating $\dot{N}_o$ in two ways: firstly $\dot{N}_o = \frac{\mathrm{d}N_o}{\mathrm{d}c_2}\dot{c}_2$, where $N_o(c_2)$ is given by

$$N_o(c_2) = \left(\frac{\varrho - \sum_{k=1}^{\infty} 2kQ_{2k}(b_2c_2/a_1)^k}{\sum_{k=1}^{\infty}(2k-1)Q_{2k-1}(b_2c_2/a_1)^{k-1}}\right)\sum_{k=1}^{\infty} Q_{2k-1}\left(\frac{b_2c_2}{a_1}\right)^{r-1}. \tag{84}$$

Secondly, (82) can be used, substituting (80) into the right-hand side to write the sum of fluxes purely as a function of c_2, using (83) to eliminate c_1.

Note that the reduction (80) can also be used to determine $c_1(t)$, $c_2(t)$ at the end of the fast phase. Since $N_o(t)$ remains constant over the fast phase, during the meta-stable timescale, $N_o(t) = N_o(0)$. Thus during the meta-stable phase, $c_1 = N_o(0)\big/\sum_{k=1}^{\infty} Q_{2k-1}(b_2c_2/a_1)^{k-1}$, with c_2 being determined by the density criterion (81).

5. Conclusion

The work of Wonczak [20] prompts the investigation into nucleation models where not only monomers interact, but also dimers. In such systems a detailed balancing condition limits the rate coefficients a_r, b_r, $\hat{a}_r$ and $\hat{b}_r$ to only three degrees of freedom. There exists a Lyapunov function when fragmentation is stronger than aggregation, forcing the system towards the unique equilibrium configuration given by the partition function. Having presented the general dimer system, the scope of this paper is restricted to the case of size-independent aggregation and fragmentation coefficients. Initially, the system is further limited to the case of a constant monomer concentration, the consequence of which is a non-constant density. If fragmentation is stronger than aggregation, we determine the equilibrium configuration and the manner in which the system approaches this state. A transition region separates equilibrated cluster sizes and those with zero concentration, and this region travels at a constant velocity towards increasingly large cluster sizes. Our results show that the speed of this transition region is increased by the presence of the dimer interaction and so the system will equilibrate faster than if only monomer interactions were permitted. Additionally, the dimer interaction broadens the width of the transition region. The far-field analysis performed supports the expression for the velocity of the transition region. The steady-state solution has a constant positive flux due to monomer interactions and a decreasing (in time) negative flux due to dimer interactions.

The equilibrium solution fails to predict a physical solution when aggregation is stronger than fragmentation and in this regime the system is found to approach a steady-state solution where mass is constantly transported to larger cluster sizes. We have determined the steady-state solution; which requires knowledge of the first correction term in order to deduce the leading-order solution. A transition region, similar to that in the equilibrium case, was found; however, the dimer interaction only broadens this region; it has no impact on its velocity. Again the far-field analysis confirms the velocity of the transition region. Certain theories, such as that proposed by Langer [22], assume that clusters aggregate to a critical size and continue to grow at the same steady rate and hence aim to evaluate this rate. We make a link

to such theories by proposing that the nucleation rate is the flux at infinite cluster size; without dimer interactions we find that $J_\infty = (ac_1 - b)c_1$. Allowing dimer interactions complicates this, in that there are then two fluxes, one due to cluster–monomer interactions (J) and one due to cluster–dimer interactions (K). The monomer flux is then $J_\infty = (ac_1 - b)c_\infty$ and the dimer flux is $K_\infty = kc_\infty(ac_2 - b)$. As $t \to \infty, c_2 \to b/a$ and therefore $K_\infty \to 0$ so that the nucleation rate is due solely to monomer–cluster, rather than dimer–cluster, interactions. Counter intuitively, since $c_\infty < c_1$ the dimer interaction reduces the monomer flux at infinity and hence reduces the nucleation rate. In the approach to the steady state, the dimer flux causes a back flow of mass to smaller aggregation numbers, an effect which decays at an anomalously small rate ($K_\infty \sim O(1/t)$ as $t \to \infty$).

The constant density system has been examined assuming a strong dimer interaction. For an example of such a system, the reader is referred to the work of Maillet *et al* [23] where micelles form with a strong influence from the dimer interaction. Two timescales were identified, initially the odd-sized clusters rapidly equilibrated, and similarly for the even-sized clusters, after which the system tends towards a global equilibrium. By considering the number of clusters of odd sizes, N_o, which is constant over the fast phase but varies over the slow timescale, we determined the intermediate meta-stable state, the final state and the timescales over which the system relaxes into these states. The fast timescale is governed by the strength of the dimer interaction whereas the slow timescale has been found to have a complex dependence on the reaction rate coefficients, the density and the final equilibrium state.

There are many directions for further work; for example, it may be instructive to consider a system with more general rate coefficients. Alternatively, the effect of trimer (three particle clusters) interactions can be investigated where the detailed balancing condition would only allow four degrees of freedom when prescribing the six reaction rate coefficients. In this case we speculate that due to $\dot{c}_2$ and $\dot{c}_3$ coupling the system together the behaviour would be both complex and rich in structure; details of this will appear in [24].

Acknowledgment

Colin Bolton is supported by an EPSRC Research Studentship.

References

[1] Becker R and Döring W 1935 *Ann. Phys., NY* **24** 719
[2] Penrose O and Lebowitz J L 1976 *Studies in Statistical Mechanics: VII. Fluctuation Phenomena* (Amsterdam: North-Holland)
[3] Ball J M, Carr J and Penrose O 1986 *Commun. Math. Phys.* **104** 657
[4] Ball J M and Carr J 1988 *Proc. R. Soc. Edin.* A **108** 109
[5] Wattis J A D and King J R 1998 *J. Phys. A: Math. Gen.* **31** 7169
[6] Penrose O 1989 *Commun. Math. Phys.* **124** 515
[7] Carr J and Dunwell R M 1999 *Proc. Edin. Math. Soc.* **42** 415
[8] Carr J, Duncan D B and Walshaw C H 1995 *IMA J. Numer. Anal.* **15** 505
[9] Duncan D B and Soheili A R 2001 *Appl. Numer. Math.* **37** 1
[10] Coveney P V and Wattis J A D 1996 *Proc. R. Soc.* A **452** 2079
[11] Coveney P V and Wattis J A D 1998 *J. Chem. Soc. Faraday Trans.* **94** 233
[12] Wattis J A D and Coveney P V 1999 *J. Phys. Chem.* B **103** 4231
[13] Wattis J A D 1999 *J. Phys. A: Math. Gen.* **32** 8755
[14] Krapivsky P L and Redner S 1996 *Phys. Rev.* E **54** 3553
[15] Wattis J A D and Coveney P V 1997 *J. Chem. Phys.* **106** 9122
[16] Krapivsky P L 1995 *Phys. Rev.* E **52** 3455

[17] von Smoluchowski M 1916 *Phys. Z* **17** 557
[18] Blackman J A and Marshall A 1994 *J. Phys. A: Math. Gen.* **27** 725
[19] Brilliantov N V and Krapivsky P L 1991 *J. Phys. A: Math. Gen.* **24** 4787
[20] Wonczak S 2002 *PhD Thesis* unpublished
[21] da Costa F P 1998 *Nonlinear Differ. Equ. Appl.* **5** 23
[22] Langer J S 1969 *Ann. Phys., NY* **54** 258–75
[23] Maillet J B, Lachet V and Coveney P V 1999 *Phys. Chem. Chem. Phys.* **1** 5277
[24] Bolton C D 2003 *PhD Thesis* Nottingham University unpublished